

# Quantum Surface-Response of Metals Revealed by Acoustic Graphene Plasmons

P. A. D. Gonçalves,<sup>1,2,\*</sup> Thomas Christensen,<sup>1</sup> Nuno M. R. Peres,<sup>3</sup> Antti-Pekka Jauho,<sup>4,5</sup> Itai Epstein,<sup>6,7</sup> Frank H. L. Koppens,<sup>6,8</sup> Marin Soljačić,<sup>1</sup> and N. Asger Mortensen<sup>2,4,9,†</sup>

<sup>1</sup>Department of Physics, Massachusetts Institute of Technology, Cambridge, MA 02139, USA

<sup>2</sup>Center for Nano Optics, University of Southern Denmark, DK-5230 Odense M, Denmark

<sup>3</sup>Department of Physics and Center of Physics, and QuantaLab, University of Minho, PT-4710-057, Braga, Portugal

<sup>4</sup>Center for Nanostructured Graphene, Technical University of Denmark, DK-2800 Kgs. Lyngby, Denmark

<sup>5</sup>Department of Physics, Technical University of Denmark, DK-2800 Kgs. Lyngby, Denmark

<sup>6</sup>ICFO — The Institute of Photonic Sciences, The Barcelona Institute of Science and Technology, 08860 Castelldefels (Barcelona), Spain

<sup>7</sup>Department of Physical Electronics, School of Electrical Engineering, Tel Aviv University, Tel Aviv 6997801, Israel

<sup>8</sup>ICREA — Institució Catalana de Recerca i Estudis Avançats, Barcelona, Spain

<sup>9</sup>Danish Institute for Advanced Study, University of Southern Denmark, DK-5230 Odense M, Denmark

A quantitative understanding of the electromagnetic response of materials is essential for the precise engineering of maximal, versatile, and controllable light–matter interactions. Material surfaces, in particular, are prominent platforms for enhancing electromagnetic interactions and for tailoring chemical processes. However, at the deep nanoscale, the electromagnetic response of electron systems is significantly impacted by quantum surface-response at material interfaces, which is challenging to probe using standard optical techniques. Here, we show how ultra-confined acoustic graphene plasmons (AGPs) in graphene–dielectric–metal structures can be used to probe the quantum surface-response functions of nearby metals, here encoded through the so-called Feibelman  $d$ -parameters. Based on our theoretical formalism, we introduce a concrete proposal for experimentally inferring the low-frequency quantum response of metals from quantum shifts of the AGPs’ dispersion, and demonstrate that the high field confinement of AGPs can resolve intrinsically quantum mechanical electronic length-scales with subnanometer resolution. Our findings reveal a promising scheme to probe the quantum response of metals, and further suggest the utilization of AGPs as plasmon rulers with ångström-scale accuracy.

Light is a prominent tool to probe the properties of materials and their electronic structure, as evidenced by the widespread use of light-based spectroscopies across the physical sciences [1, 2]. Among these tools, far-field optical techniques are particularly prevalent, but are constrained by the diffraction limit and the mismatch between optical and electronic length scales to probe the response of materials only at large length scales (or, equivalently, at small momenta). Plasmon polaritons—hybrid excitations of light and free carriers—provide a mean to overcome these constraints through their ability to confine electromagnetic radiation to the nanoscale [3]. Graphene, in particular, supports gate-tunable plasmons characterized by an unprecedentedly strong confinement of light [4–6]. When placed near a metal, graphene plasmons (GPs) are strongly screened and acquire a nearly-linear (acoustic-like) dispersion [7–10] (contrasting with the square-root-type dispersion of conventional GPs). Crucially, such acoustic graphene plasmons (AGPs) in graphene–dielectric–metal (GDM) structures have been shown to exhibit even higher field confinement than conventional GPs with the same frequency, effectively squeezing light into the few-nanometer regime [8–11]. Recently, using scanning near-field optical microscopy, these features were exploited to experimentally measure the conductivity of graphene,  $\sigma(q, \omega)$ , across its frequency ( $\omega$ ) and momentum ( $q$ ) dependence simultaneously [8]. The observation of momentum-dependence implies a nonlocal response (i.e., response contributions at position  $\mathbf{r}$  from perturbations at  $\mathbf{r}'$ ), whose origin is inherently quantum mechanical. Incidentally, traditional optical spectroscopic tools cannot resolve nonlocal response in extended systems due to the intrinsically small momenta  $k_0 \equiv \omega/c$  carried by far-field photons. Acoustic graphene plasmons, on the other hand, can carry large

momenta—even asymptotically approaching the electronic Fermi momentum  $k_F$ —and so can facilitate explorations of nonlocal (i.e.,  $q$ -dependent) response not only in graphene itself, but also, as we detail in this Article, in nearby materials. So far, however, only aspects related to the quantum response of graphene have been addressed [8], leaving any quantum nonlocal aspects of the adjacent metal’s response unattended, despite their potentially substantial impact at nanometric graphene–metal separations [12–16].

Here, we present a theoretical framework that simultaneously incorporates quantum nonlocal effects in the response of both the graphene and of the metal substrate for AGPs in GDM heterostructures. Further, our approach establishes a concrete proposal for experimentally measuring the low-frequency nonlocal electrodynamic response of metals. Our model treats graphene at the level of the nonlocal random-phase approximation (RPA) [4, 9, 17–19] and describes the quantum aspects of the metal’s response—including nonlocality, electronic spill-out/spill-in, and surface-enabled Landau damping—using a set of microscopic surface-response functions known as the Feibelman  $d$ -parameters [12, 13, 15, 16, 20, 21]. These parameters,  $d_{\perp}$  and  $d_{\parallel}$ , measure the frequency-dependent centroids of the induced charge density and of the normal derivative of the tangential current density, respectively (Supplementary Section S1). Using a combination of numerics and perturbation theory, we show that the AGPs are spectrally shifted by the quantum surface-response of the metal: toward the red for  $\text{Re } d_{\perp} > 0$  (associated with electronic spill-out of the induced charge density) and toward the blue for  $\text{Re } d_{\perp} < 0$  (signaling an inward shift, or “spill-in”). Interestingly, these shifts are not accompanied by a commensurately large quantum broadening nor by a reduction of the AGP’s quality factor, thereby

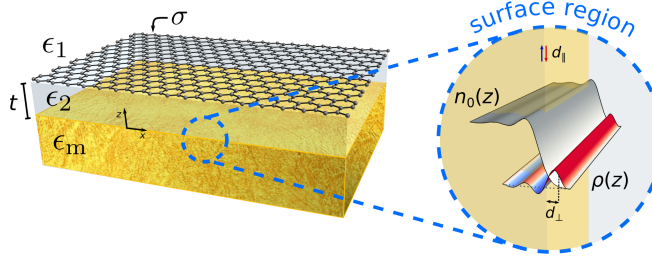


**Figure 1. Schematics of a dielectric-graphene-dielectric-metal (GDM) heterostructure.** The graphene–metal separation,  $t$ , is controlled by the thickness of the dielectric ( $\epsilon_2$ ) spacer. The close-up (near the metal–spacer interface) shows a pictorial representation of the surface-response functions  $d_{\perp}$  and  $d_{\parallel}$  along with the related microscopic quantities characterizing the metal surface, namely the equilibrium electronic density,  $n_0(z)$ , and the induced charge density,  $\rho(z)$ .

providing the theoretical support explaining recent experimental observations [11]. Finally, we discuss how state-of-the-art measurements of AGPs could be leveraged to map out the low-frequency quantum nonlocal surface-response of metals.

## RESULTS

We consider a GDM heterostructure (see Fig. 1) composed of a graphene sheet with a surface conductivity  $\sigma \equiv \sigma(q, \omega)$

separated from a metal substrate by a thin dielectric slab of thickness  $t$  and relative permittivity  $\epsilon_2 \equiv \epsilon_2(\omega)$ ; finally, the device is covered by a superstrate of relative permittivity  $\epsilon_1 \equiv \epsilon_1(\omega)$ . While the metal substrate may, in principle, be represented by a nonlocal and spatially non-uniform (near the interface) dielectric function, here we abstract its contributions into two parts: a bulk, local contribution via  $\epsilon_m \equiv \epsilon_m(\omega) = \epsilon_\infty(\omega) - \omega_p^2/(\omega^2 + i\omega\gamma_m)$ , and a surface, quantum contribution included through the  $d$ -parameters.

The electromagnetic excitations of any system can be obtained by analyzing the poles of the (composite) system's scattering coefficients. For the AGPs of a GDM structure, the relevant coefficient is the  $p$ -polarized reflection (or transmission) coefficient, whose poles are given by  $1 - r_p^{2|g|1} r_p^{2|m} e^{i2k_{z,2}t} = 0$  [22]. Here,  $r_p^{2|g|1}$  and  $r_p^{2|m}$  denote the  $p$ -polarized reflection coefficients for the dielectric–graphene–dielectric and the dielectric–metal interface (both with incidence from  $\epsilon_2$ ), respectively. Each coefficient yields a material-specific contribution to the overall quantum response:  $r_p^{2|g|1}$  incorporates graphene's via  $\sigma(q, \omega)$ , and  $r_p^{2|m}$  incorporates the metal's via the  $d$ -parameters (see Supplementary Section S2). The complex exponential [with  $k_{z,2} \equiv (\epsilon_2 k_0^2 - q^2)^{1/2}$ , where  $q$  denotes the in-plane wavevector] incorporates the effects of multiple reflections within the slab. Thus, using the above-noted reflection coefficients (defined explicitly in the Supplementary Section S2), we obtain a quantum-corrected AGP dispersion equation:

$$\left[ \frac{\epsilon_1}{\kappa_1} + \frac{\epsilon_2}{\kappa_2} + \frac{i\sigma}{\omega\epsilon_0} \right] \left[ \epsilon_m \kappa_2 + \epsilon_2 \kappa_m - (\epsilon_m - \epsilon_2)(q^2 d_{\perp} - \kappa_2 \kappa_m d_{\parallel}) \right] = \left[ \frac{\epsilon_1}{\kappa_1} - \frac{\epsilon_2}{\kappa_2} + \frac{i\sigma}{\omega\epsilon_0} \right] \left[ \epsilon_m \kappa_2 - \epsilon_2 \kappa_m + (\epsilon_m - \epsilon_2)(q^2 d_{\perp} + \kappa_2 \kappa_m d_{\parallel}) \right] e^{-2\kappa_2 t}, \quad (1)$$

for in-plane AGP wavevector  $q$  and out-of-plane confinement factors  $\kappa_j \equiv \sqrt{q^2 - \epsilon_j k_0^2}$  for  $j \in \{1, 2, m\}$ .

Since AGPs are exceptionally subwavelength (with confinement factors up to almost 300) [8, 10, 11], the nonretarded limit (wherein  $\kappa_j \rightarrow q$ ) is an excellent approximation. In this regime, and for encapsulated graphene, i.e., where  $\epsilon_d \equiv \epsilon_1 = \epsilon_2$ , Eq. (1) simplifies to

$$\left[ 1 + \frac{2\epsilon_d}{q} \frac{\omega\epsilon_0}{i\sigma} \right] \left[ \frac{\epsilon_m + \epsilon_d}{\epsilon_m - \epsilon_d} - q(d_{\perp} - d_{\parallel}) \right] = \left[ 1 + q(d_{\perp} + d_{\parallel}) \right] e^{-2qt}. \quad (2)$$

The quantum surface-response functions  $d_{\alpha}$  (with  $\alpha = \{\perp, \parallel\}$ ) can be either computed (e.g., with time-dependent density functional theory or from semiclassical nonlocal models [13, 20, 21]) or obtained from experimental data [15]. For simplicity and concreteness, we will consider a simple jellium treatment of the metal such that  $d_{\parallel}$  vanishes due to charge neutrality [21, 24], leaving only  $d_{\perp}$  nonzero. Next, we exploit the fact that AGPs typically span frequencies across the tera-

hertz (THz) and mid-infrared (mid-IR) ranges, i.e., well below the plasma frequency  $\omega_p$  of the metal. In this low-frequency regime,  $\omega \ll \omega_p$ , the frequency-dependence of  $d_{\perp}$  (and  $d_{\parallel}$ ) has the universal, asymptotic dependence

$$d_{\perp}(\omega) \simeq \zeta + i \frac{\omega}{\omega_p} \xi \quad (\text{for } \omega \ll \omega_p), \quad (3)$$

as shown by Persson et al. [23, 25] by exploiting Kramers–Kronig relations. Here,  $\zeta$  is the so-called static image-plane position, i.e., the centroid of induced charge under a static, external field [26]; and  $\xi$  defines a phase-space coefficient for low-frequency electron–hole pair creation, whose rate is  $\propto q\omega\xi$  [21]; both are ground-state quantities. In the jellium approximation of the interacting electron liquid, the constants  $\zeta \equiv \zeta(r_s)$  and  $\xi \equiv \xi(r_s)$  depend solely on the carrier density  $n_e$ , here parameterized by the Wigner–Seitz radius  $r_s a_B \equiv (3n_e/4\pi)^{1/3}$  (Bohr radius,  $a_B$ ). In the following, we exploit the simple asymptotic relation in Eq. (3) to calculate the dispersion of AGPs with metallic (in addition to graphene's) quantum response

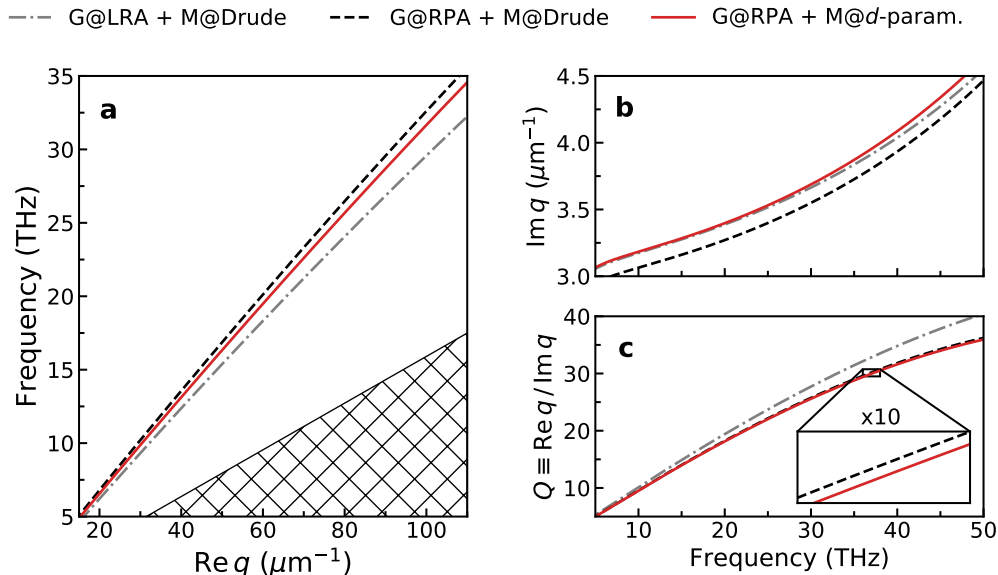


**Figure 2. Influence of metallic quantum surface-response on the dispersion of acoustic graphene plasmons (AGPs).** Three increasingly sophisticated tiers of response models are considered: (i) classical, local response for both the graphene and the metal [gray dot-dashed line]; (ii) nonlocal RPA and local Drude response for the graphene and the metal, respectively [black dashed line]; and (iii) nonlocal RPA and  $d$ -parameter-augmented response for the graphene and the metal, respectively [red solid line]. **a**, AGP dispersion diagram,  $\omega/(2\pi)$  versus  $\text{Re } q$ . The hatched region indicates the graphene's electron–hole continuum. **b**, Associated imaginary part of the AGP wavevector,  $\text{Im } q$ . **c**, Corresponding quality factor  $Q \equiv \text{Re } q / \text{Im } q$ . The inset shows a  $10\times$  zoom of the indicated region. System parameters: we take a graphene–metal separation of  $t = 1 \text{ nm}$ ; for concreteness and simplicity, we consider an unscreened jellium metal with plasma frequency  $\hbar\omega_p \approx 9.07 \text{ eV}$  (corresponding to  $r_s = 3$ ) where  $\zeta \approx 0.8 \text{ \AA}$  and  $\xi \approx 0.3 \text{ \AA}$  [23], with Drude-type damping  $\hbar\gamma_m = 0.1 \text{ eV}$ ; for graphene, we take  $E_F = 0.3 \text{ eV}$  and  $\hbar\gamma = 8 \text{ meV}$ ; finally, we have assumed  $\epsilon_d \equiv \epsilon_1 = \epsilon_2 = 1$  (for consistency with the  $d$ -parameter data which assumes a metal–vacuum interface [23]).

included.

The spectrum of AGPs calculated classically and with quantum corrections is shown in Figure 2. Three models are considered: one, a classical, local-response approximation (LRA) treatment of both the graphene and the metal; and two others, in which graphene's response is treated by the nonlocal RPA [4, 9, 17–19] while the metal's response is treated either classically or with quantum surface-response included (via the  $d_{\perp}$ -parameter). Figure 2a shows that—for a fixed wavevector—the AGP's resonance redshifts relative to the classical result for jellium metals where  $\text{Re } d_{\perp} > 0$  (electronic spill-out) [13, 15, 16, 21, 27, 28]. This behavior is the opposite to that predicted by the semiclassical hydrodynamic model (HDM) where the result is always a blueshift [14] (corresponding to  $\text{Re } d_{\perp}^{\text{HDM}} < 0$ ) due to the neglect of spill-out effects [29]. The imaginary part of the AGP's wavevector (that characterizes the mode's propagation length) is shown in Fig. 2b: the net effect of  $d_{\perp}$ 's inclusion is a small, albeit consistent, increase of this imaginary component. Notwithstanding, the modification of  $\text{Im } q$  is not independent of the shift in  $\text{Re } q$ ; as a result, an increase in  $\text{Im } q$  does not necessarily imply the presence of a significant quantum decay channel [e.g., an increase of  $\text{Im } q$  can simply result from increased *classical* loss (i.e., arising from local-response alone) at the newly shifted  $\text{Re } q$  position]. Because of this, we inspect the quality factor  $Q \equiv \text{Re } q / \text{Im } q$

instead (Fig. 2c), which provides a complementary perspective that emphasizes the *effective* (or normalized) propagation length rather than the absolute length. The incorporation of quantum mechanical effects, first in graphene alone, and then in both graphene and metal, reduces the AGP's quality factor. Still, the impact of metal-related quantum losses in the latter is negligible, as evidenced by the nearly overlapping black and red curves in Fig. 2c.

To better understand these observations, we treat the AGP's  $q$ -shift due to the metal's quantum surface-response as a perturbation: writing  $q = q_0 + q_1$ , we find that the quantum correction from the metal is  $q_1 \simeq q_0 d_{\perp} / (2t)$ , for a jellium adjacent to vacuum in the  $\omega^2/\omega_p^2 \ll q_0 t \ll 1$  limit (Supplementary Section S3A). This simple result, together with Eq. (3), provides a near-quantitative account of the AGP dispersion shifts due to metallic quantum surface-response: for  $\omega \ll \omega_p$ , (i)  $\text{Re } d_{\perp}$  tends to a finite value,  $\zeta$ , which increases (decreases)  $\text{Re } q$  for  $\zeta > 0$  ( $\zeta < 0$ ); and (ii)  $\text{Im } d_{\perp}$  is  $\propto \omega$  and therefore asymptotically vanishing as  $\omega/\omega_p \rightarrow 0$  and so only negligibly increases  $\text{Im } q$ . Moreover, the preceding perturbative analysis warrants  $\text{Re } q_1 / \text{Re } q_0 \approx \text{Im } q_1 / \text{Im } q_0$  (Supplementary Section S3A), which elucidates the reason why the AGP's quality factor remains essentially unaffected by the inclusion of metallic quantum surface-response. These results explain recent experimental observations that found appreciable spectral shifts

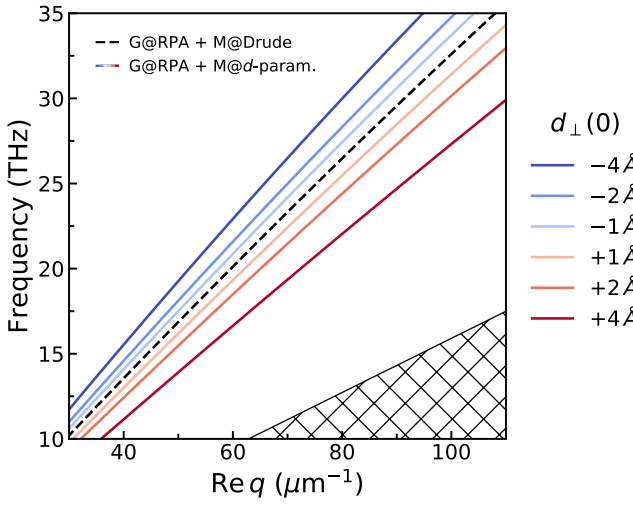


**Figure 3. Concept for using the spectral shifting of AGPs for retrieving the quantum surface-response of metals.** Impact of  $d_{\perp}(\omega \ll \omega_p) \simeq d_{\perp}(0) \equiv \zeta$  on the AGP's dispersion [obtained through the numerical solution of Eq. (1)]. All parameters (with the exception of  $d_{\perp}$ ) are the same as in Fig. 2.

but negligible additional broadening due to quantum response in the metallic substrate [11].

Next, by considering the separation between graphene and the metallic interface as a renormalizable parameter, we find a complementary and instructive perspective on the impact of metallic quantum surface-response. Specifically, within the spectral range of interest for AGPs (i.e.,  $\omega \ll \omega_p$ ), we find that the “bare” graphene–metal separation  $t$  is effectively renormalized due to the metal’s quantum surface-response from  $t$  to  $\tilde{t} \equiv t - s$ , where  $s \simeq d_{\perp} \simeq \zeta$  (see Supplementary Section S3B), corresponding to a physical picture where the metal’s interface lies at the centroid of its induced density (i.e.,  $\text{Re } d_{\perp}$ ) rather than at its “classical” jellium edge. With this approach, the form of the dispersion equation is unchanged but references the renormalized separation  $\tilde{t}$  instead of its bare counterpart  $t$ , i.e.:

$$1 + \frac{2\epsilon_d}{q} \frac{\omega\epsilon_0}{i\sigma} = \frac{\epsilon_m - \epsilon_d}{\epsilon_m + \epsilon_d} e^{-2q\tilde{t}}, \quad (4)$$

This perspective, for instance, has substantial implications for the analysis and understanding of plasmon rulers [30–32] at nanometric scales.

Furthermore, our findings additionally suggest an interesting experimental opportunity: as all other experimental parameters can be well-characterized by independent means (including the nonlocal conductivity of graphene), high-precision measurements of the AGP dispersion can enable the characterization of the low-frequency metallic quantum response—a regime that has otherwise been inaccessible in conventional metal-only plasmonics. The underlying idea is illustrated in Fig. 3; depending on the sign of the static asymptote  $\zeta \equiv d_{\perp}(0)$ , the AGP dispersion shifts toward larger  $q$  (smaller  $\omega$ ; redshift) for  $\zeta > 0$  and toward smaller  $q$  (larger  $\omega$ ; blueshift) for  $\zeta < 0$ . As noted

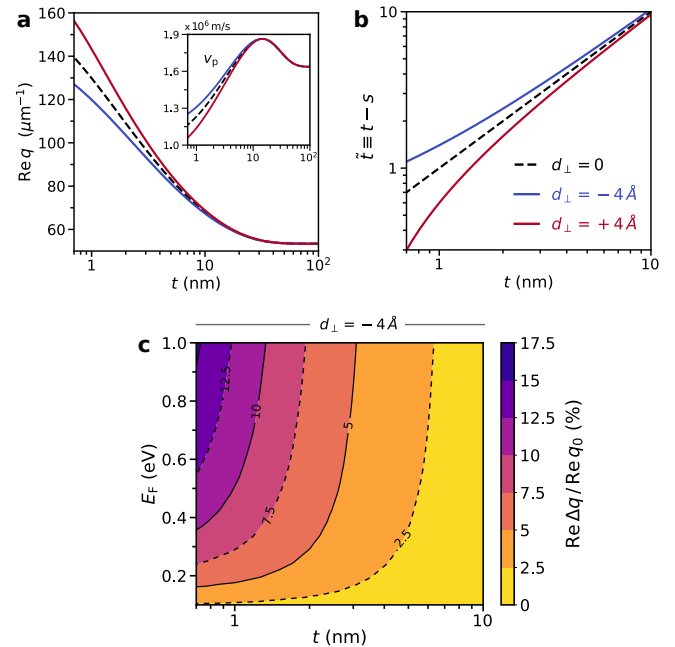


**Figure 4. Nonclassical corrections probed by AGPs.** **a**, AGP's wavevector as a function of the graphene–metal separation  $t$ , contrasting the metal's response based on classical ( $d_{\perp} = 0$ ) and quantum ( $d_{\perp} = \pm 4 \text{ \AA}$ ) treatments. Inset: corresponding group velocity  $v_p = \partial\omega/\partial q|_{q=q(\omega_0)}$ . **b**, Dependence of the renormalized graphene–metal separation  $\tilde{t} \equiv t - s$  versus  $t$ . Setup parameters:  $r_s = 3$ ,  $\hbar\gamma_m = 0.1 \text{ eV}$ ,  $\epsilon_d = 4$ ,  $E_F = 0.3 \text{ eV}$  and  $\hbar\gamma = 8 \text{ meV}$ ; we assume an excitation at  $\lambda_0 = 11.28 \mu\text{m}$  ( $\hbar\omega_0 \approx 110 \text{ meV}$  or  $f_0 \approx 26.6 \text{ THz}$ ) [33]. **c**, Relative quantum shift of the AGP wavevector,  $\text{Re } \Delta q / \text{Re } q_0$ , with  $\Delta q \equiv q_0 - q$  where  $q_0$  and  $q$  denote the AGP wavevector associated with  $d_{\perp} = 0$  and  $d_{\perp} = -4 \text{ \AA}$ , respectively. The results presented in both **a** and **c** are based on the exact, numerical solution of Eq. (1).

above, the  $q$ -shift is  $\sim q_0\zeta/(2t)$ . Crucially, despite the ångström-scale of  $\zeta$ , this shift can be sizable: the inverse scaling with the spacer thickness  $t$  effectively amplifies the attainable shifts in  $q$ , reaching up to several  $\mu\text{m}^{-1}$  for few-nanometer  $t$ . We stress that these regimes are well within current state-of-the-art experimental capabilities [8, 10, 11], suggesting a new path toward the systematic exploration of the static quantum response of metals.

The key parameter that regulates the impact of quantum surface corrections stemming from the metal is the graphene–metal separation,  $t$  (analogously to the observations of nonclassical effects in conventional plasmons at narrow metal gaps [13, 34, 35]); see Fig. 4. For the experimentally-representative parameters indicated in Fig. 4, these come into effect for  $t \lesssim 5 \text{ nm}$ , growing rapidly upon decreasing the graphene–metal separation further. Chiefly, ignoring the nonlocal response of the metal leads to a consistent overestimation (underestimation) of AGP’s wavevector (group velocity) for  $d_{\perp} < 0$ , and vice-versa for  $d_{\perp} > 0$  (Fig. 4a); this behavior is consistent with the effective renormalization of the graphene–metal separation mentioned earlier (Fig. 4b). Fi-

nally, we analyze the interplay of both  $t$  and  $E_F$  and their joint influence on the magnitude of the quantum corrections from the metal (we take  $d_\perp = -4 \text{ \AA}$ , which is reasonable for the Au substrate used in recent AGP experiments [7, 8, 11]); in Fig. 4c we show the relative wavevector quantum shift (excited at  $\lambda_0 = 11.28 \mu\text{m}$  [33]). In the few-nanometer regime, the quantum corrections to the AGP wavevector approach 5%, increasing further as  $t$  decreases—for instance, in the extreme, one-atom-thick limit ( $t \approx 0.7 \text{ nm}$  [11], which also approximately coincides with edge of the validity of the  $d$ -parameter framework, i.e.,  $t \gtrsim 1 \text{ nm}$  [15]) the AGP's wavevector can change by as much as 10% for moderate graphene doping.

## DISCUSSION

In this Article, we have presented a theoretical account that establishes and quantifies the influence of the metal's quantum response for AGPs in hybrid graphene–dielectric–metal structures. We have demonstrated that the nanoscale confinement of electromagnetic fields inherent to AGPs can be harnessed to determine the quantum surface-response of metals in the THz and mid-IR spectral ranges. In particular, our formalism provides a transparent theoretical foundation for guiding experimental measurements of the quantum surface-response of metals using AGPs.

The knowledge of the metal's low-frequency, static quantum response is of practical utility in a plethora of scenarios, enabling, for instance, the incorporation of leading-order quantum corrections to the classical electrostatic image theory of particle–surface interaction [20] as well as to the van der Waals interaction [21, 25, 36] affecting atoms or molecules near metal surfaces. Our findings also highlight that AGPs can be extremely sensitive probes for nanometrology as plasmon rulers, while simultaneously underscoring the importance of incorporating quantum response in the characterization of such rulers at (sub)nanometric scales. Finally, the theory introduced here further suggests new directions for exploiting AGP's high-sensitivity, e.g., to explore the physics governing the complex electron dynamics at the surfaces of a superconductors [37] and other strongly-correlated systems.

**Acknowledgements** — N. A. M. is a VILLUM Investigator supported by VILLUM FONDEN (Grant No. 16498). The Center for Nano Optics is financially supported by the University of Southern Denmark (SDU 2020 funding). The Center for Nanostructured Graphene (CNG) is sponsored by the Danish National Research Foundation (Project No. DNRF103). This work was partly supported by the Army Research Office through the Institute for Soldier Nanotechnologies under contract No. W911NF-18-2-0048. N. M. R. P. acknowledges support from the European Commission through the project “Graphene-Driven Revolutions in ICT and Beyond” (No. 881603, Core 3) and COMPETE 2020, PORTUGAL 2020, FEDER and the Portuguese Foundation for Science and Technology (FCT) through project POCI-01-0145-FEDER-028114. F. H. L. K. acknowledges financial support from the Government of Catalonia through the SGR grant and from the Spanish Ministry of Economy and Competitiveness through the Severo Ochoa Programme for Centres of Excellence in

R&D (SEV-2015-0522), support by Fundació Cellex Barcelona, Generalitat de Catalunya through the CERCA program, and the Mineco grants Plan Nacional (FIS2016-81044-P) and the Agency for Management of University and Research Grants (AGAUR) 2017 SGR 1656. Furthermore, the research leading to these results has received funding from the European Union's Horizon 2020 program under the Graphene Flagship grant agreements No. 785219 (Core 2) and No. 881603 (Core 3), and the Quantum Flagship grant No. 820378. This work was also supported by the ERC TOPONANOP under grant agreement No. 726001.

## REFERENCES

\* pa@mci.sdu.dk

† asger@mailaps.org

- [1] N. Tkachenko, *Optical Spectroscopy: Methods and Instrumentations*, 1st ed. (Elsevier, 2006).
- [2] J. M. Hollas, *Modern Spectroscopy*, 4th ed. (Wiley, 2004).
- [3] D. K. Gramotnev and S. I. Bozhevolnyi, *Nat. Photonics* **4**, 83 (2010).
- [4] P. A. D. Gonçalves and N. M. R. Peres, *An Introduction to Graphene Plasmonics*, 1st ed. (World Scientific, Singapore, 2016).
- [5] F. H. L. Koppens, D. E. Chang, and F. J. García de Abajo, *Nano Lett.* **11**, 3370 (2011).
- [6] F. J. García de Abajo, *ACS Photonics* **1**, 135 (2014).
- [7] P. Alonso-González, A. Y. Nikitin, Y. Gao, A. Woessner, M. B. Lundeberg, A. Principi, N. Forcellini, W. Yan, S. Vélez, A. J. Huber, K. Watanabe, T. Taniguchi, F. Casanova, L. E. Hueso, M. Polini, J. Hone, F. H. L. Koppens, and R. Hillenbrand, *Nat. Nanotechnol.* **12**, 31 (2017).
- [8] M. B. Lundeberg, Y. Gao, R. Asgari, C. Tan, B. Van Duppen, M. Autore, P. Alonso-González, A. Woessner, K. Watanabe, T. Taniguchi, R. Hillenbrand, J. Hone, M. Polini, and F. H. L. Koppens, *Science* **357**, 187 (2017).
- [9] P. A. D. Gonçalves, *Plasmonics and Light–Matter Interactions in Two-Dimensional Materials and in Metal Nanostructures: Classical and Quantum Considerations* (Springer Nature, 2020).
- [10] I. Epstein, D. Alcaraz, Z. Huang, V.-V. Pusapati, J.-P. Hugonin, A. Kumar, X. M. Deputy, T. Khodkov, T. G. Rappoport, J.-Y. Hong, N. M. R. Peres, J. Kong, D. R. Smith, and F. H. L. Koppens, *Science* **368**, 1219 (2020).
- [11] D. Alcaraz Iranzo, S. Nanot, E. J. C. Dias, I. Epstein, C. Peng, D. K. Efetov, M. B. Lundeberg, R. Parret, J. Osmond, J.-Y. Hong, J. Kong, D. R. Englund, N. M. R. Peres, and F. H. L. Koppens, *Science* **360**, 291 (2018).
- [12] W. Yan, M. Wubs, and N. A. Mortensen, *Phys. Rev. Lett.* **115**, 137403 (2015).
- [13] T. Christensen, W. Yan, A.-P. Jauho, M. Soljačić, and N. A. Mortensen, *Phys. Rev. Lett.* **118**, 157402 (2017).
- [14] E. J. C. Dias, D. A. Iranzo, P. A. D. Gonçalves, Y. Hajati, Y. V. Bludov, A.-P. Jauho, N. A. Mortensen, F. H. L. Koppens, and N. M. R. Peres, *Phys. Rev. B* **97**, 245405 (2018).
- [15] Y. Yang, D. Zhu, W. Yan, A. Agarwal, M. Zheng, J. D. Joannopoulos, P. Lalanne, T. Christensen, K. K. Berggren, and M. Soljačić, *Nature* **576**, 248 (2019).
- [16] P. A. D. Gonçalves, T. Christensen, N. Rivera, A.-P. Jauho, N. A. Mortensen, and M. Soljačić, *Nat. Commun.* **11**, 366 (2020).
- [17] B. Wunsch, T. Stauber, F. Sols, and F. Guinea, *New J. Phys.* **8**, 318 (2006).
- [18] E. H. Hwang and S. Das Sarma, *Phys. Rev. B* **75**, 205418 (2007).

- [19] M. Jablan, H. Buljan, and M. Soljačić, *Phys. Rev. B* **80**, 245435 (2009).
- [20] P. J. Feibelman, *Prog. Surf. Sci.* **12**, 287 (1982).
- [21] A. Liebsch, *Electronic excitations at metal surfaces* (Springer, New York, 1997).
- [22] W. C. Chew, *Waves and Fields in Inhomogenous Media* (Wiley-IEEE Press, 1995).
- [23] B. N. J. Persson and P. Apell, *Phys. Rev. B* **27**, 6058 (1983).
- [24] P. Apell, *Physica Scripta* **24**, 795 (1981).
- [25] B. N. J. Persson and E. Zaremba, *Phys. Rev. B* **40**, 5669 (1984).
- [26] N. D. Lang and W. Kohn, *Phys. Rev. B* **7**, 3541 (1973).
- [27] A. Liebsch, *Phys. Rev. B* **36**, 7378 (1987).
- [28] A. Liebsch, *Phys. Rev. B* **48**, 11317 (1993).
- [29] S. Raza, S. I. Bozhevolnyi, M. Wubs, and N. A. Mortensen, *J. Phys.: Condens. Matter* **27**, 183204 (2015).
- [30] C. Sönnichsen, B. M. Reinhard, J. Liphardt, and A. P. Alivisatos, *Nat. Biotechnol.* **23**, 741 (2005).
- [31] R. T. Hill, J. J. Mock, A. Hucknall, S. D. Wolter, N. M. Jokerst, D. R. Smith, and A. Chilkoti, *ACS Nano* **6**, 9237 (2012).
- [32] T. V. Teperik, P. Nordlander, J. Aizpurua, and A. G. Borisov, *Phys. Rev. Lett.* **110**, 263901 (2013).
- [33] G. X. Ni, A. S. McLeod, Z. Sun, L. Wang, L. Xiong, K. W. Post, S. S. Sunku, B.-Y. Jiang, J. Hone, C. R. Dean, M. M. Fogler, and D. N. Basov, *Nature* **557**, 530 (2018).
- [34] W. Zhu, R. Esteban, A. G. Borisov, J. J. Baumberg, P. Nordlander, H. J. Lezec, J. Aizpurua, and K. B. Crozier, *Nat. Commun.* **7**, 11495 (2016).
- [35] S. Raza, T. Christensen, M. Wubs, S. I. Bozhevolnyi, and N. A. Mortensen, *Phys. Rev. B* **88**, 115401 (2013).
- [36] E. Zaremba and W. Kohn, *Phys. Rev. B* **13**, 2270 (1976).
- [37] A. T. Costa, P. A. D. Gonçalves, F. H. L. Koppens, D. N. Basov, N. A. Mortensen, and N. M. R. Peres, *arXiv:2006.00748* (2020).